Cold Regions Science and Technology 62 (2010) 119–125

Contents lists available at ScienceDirect

Cold Regions Science and Technology

journal homepage: www.elsevier.com/locate/coldregions

Load-controlled test apparatus for snow

Ingrid Reiweger [a,*], Jürg Schweizer [a], Robert Ernst [a,b], Jürg Dual [b]

[a] WSL Institute for Snow and Avalanche Research SLF, Davos, Switzerland
[b] Institute of Mechanical Systems, ETH Zürich, Switzerland

ARTICLE INFO

Article history:
Received 26 January 2010
Accepted 3 April 2010

Keywords:
Snow
Avalanche
Mechanical properties
Acoustic emissions
Strength
Particle image velocimetry

ABSTRACT

Natural dry-snow slab avalanches start with a failure at a weak snow layer. In order to understand the mechanical behaviour and the failure mechanism, we designed an experimental setup to perform loading experiments with homogeneous and layered snow samples under controlled conditions in a cold laboratory. We here present our loading apparatus where the snow sample can be tilted by a "slope angle" and is loaded by an increasing weight analogous to a snowfall. The force and the global displacement are measured with a force and two displacement sensors, respectively. The local displacement can be computed with a particle image velocimetry algorithm (PIV). Additionally, we record acoustic emissions (AE) to monitor the damage (breaking of bonds) in the snow sample before catastrophic failure. To demonstrate the capability of the system we present preliminary results with both homogeneous and layered snow samples. The AE count rate increased before fracture, as the samples progressively weakened. For the layered samples we measured a concentration of strain within the weak layer.

© 2010 Elsevier B.V. All rights reserved.

1. Introduction

We present a new loading apparatus for studying catastrophic snow failure with respect to the release of dry-snow slab avalanches. Dry-snow slab avalanches start with a failure at a weak snow layer below a cohesive slab of ample thickness (e.g. Schweizer et al., 2003). If the initial failure reaches a sufficiently large size and the snowpack conditions are favourable for crack propagation, the initial crack can propagate and an avalanche may release. While the formation of the initial failure is well understood and documented in the case of artificially triggered dry-snow slab avalanches (e.g. van Herwijnen and Jamieson, 2005), the initiation process for spontaneous dry-snow slab avalanches remains unclear. As monitoring the iniation process in the field is very challenging (e.g. van Herwijnen and Schweizer, 2008) it is best studied experimentally in a cold laboratory.

Previous studies on snow failure used deformation-controlled shear experiments (e.g. Joshi et al., 2006; Schweizer, 1998; Fukuzawa and Narita, 1993; de Montmollin, 1982; McClung, 1977). Deformation-controlled experiments give insight into the material behaviour before fracture. Depending on snow type and temperature these deformation-controlled studies typically showed brittle behaviour of snow at strain rates faster than about $10^{-3}\,s^{-1}$ and ductile behaviour at smaller strain rates. However, to study fracture itself, and in particular the processes that lead to fracture, load-controlled (or force-controlled) experiments are needed. Camponovo and Schweizer (2001) performed stress-ramp experiments with homogeneous snow with a rheometer, where the snow samples were sheared by rotation. They found that sintering of snow continuously occurred during the experiments, and only at a high applied stress did the damage process exceed the healing process. In our apparatus, the snow samples are loaded via the gravitational force. This gives a natural combination of shear and normal load depending on the "slope angle". The only other load-controlled shear experiments, to our knowledge, were performed just recently by Podolsky et al. (2008) who used a similar loading principle to pull a shear frame on a horizontal snow sample with constantly increasing force. They found that snow strength dramatically decreased with increasing loading rate.

Since for layered snow the deformation (strain) during loading is assumed to be concentrated in the weak layer or at least to be unequally distributed within the snowpack (Jamieson and Schweizer, 2000; Fukuzawa and Narita, 1993; McClung, 1987), monitoring the displacement field on the side of a layered snow sample is crucial for understanding the failure behaviour. Under the assumption of plane strain, the displacement field on the side of a sample is representative for the displacement (and thereby deformation) field within the sample. In order to measure displacement fields on snow, particle image velocimetry (PIV) has proven to be a suitable technique since it is non invasive and snow can be, depending on the snow type, very fragile. PIV was already used by Gleason (2004) who measured the deformation on snow under compression. Borstad and McClung (2004) combined high speed video images with a particle tracking software to analyze three-point-bending tests with snow specimens, while van Herwijnen and Jamieson (2005) used this combination to study crack propagation in weak snowpack layers in the field.

* Corresponding author.
E-mail address: reiweger@slf.ch (I. Reiweger).

0165-232X/$ – see front matter © 2010 Elsevier B.V. All rights reserved.
doi:10.1016/j.coldregions.2010.04.002

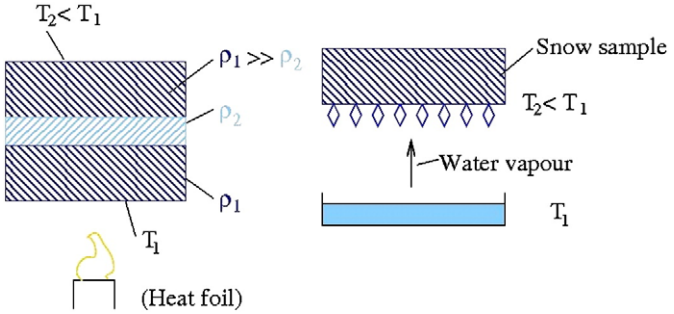

Fig. 1. Experimental setup for producing a layer of faceted crystals (left) and surface hoar (right). T denotes temperature and ρ denotes density.

One method to assess the processes leading to catastrophic failure (breaking of bonds, generation of microcracks) are acoustic emission (AE) measurements. In ice, AE were related to fracture by e.g. Cole and Dempsey (2004), who studied the breakup of sea ice. Sommerfeld and Gubler (1983) were the first to measure acoustic emissions in snow and relate them to avalanche release. They performed field studies and focused on low frequency sensors with frequencies of the order of 100 Hz because of the strong attenuation of high frequencies in snow. McClung (1987) measured acoustic emissions during slow deformation-controlled shear experiments (without catastrophic failure) in the laboratory, in the frequency range of several Hz to several kHz. Scapozza et al. (2004) measured acoustic emissions during triaxial compression tests, finding that for ductile failure behaviour the AE rate initially increased but decreased after the yield point. St. Lawrence (1980) considered snow as ice with a low density and hypothesised that the acoustic sources in snow were the same as in ice.

The aim of this paper is to present an innovative experimental setup (and demonstrate its capability) suitable for studying the processes that lead to catastrophic fracture of layered snow. The setup includes a loading apparatus, a PIV method to measure local displacement, an acoustic measuring system to estimate the microscopic failure (breaking of bonds) before final fracture, and a method for producing layered snow samples in the laboratory.

2. Methods

2.1. Production of snow samples

Snow samples were taken from the field or produced in the laboratory. Whereas field samples are fast to obtain during winter, grown samples are more easily controlled (greater reproducibility) and season independent.

For the production of homogeneous snow samples, we took new snow produced by a snow machine (Meier, 2006), sieved it into a box (2 mm grid sieve), compressed it by a defined short distance, and let it sinter one to two days at −6 °C. The resulting grains were small rounded particles. Reproducibility was checked with snow micro-penetrometer measurements. The stronger the compression and the longer the sintering, the denser, harder, and stiffer the resulting snow samples became. The densities which could be achieved this way ranged from 100 to 500 kg m^{-3}.

Considering avalanche release, snow samples containing a weak layer (e.g. faceted crystals or buried surface hoar) are more relevant than homogeneous snow samples. In the cold laboratory, weak layers of faceted crystals and depth hoar were grown by applying a strong vertical temperature gradient to a snow sample as described by Fukuzawa and Narita (1993). Our snow samples for growing faceted crystals consisted of a layer of low density snow (fresh new snow crystals produced by the snow machine) sandwiched between two dense snow layers ($\rho \approx 300$ kg m^{-3}); produced similarly as the homogeneous samples described above.

Surface hoar layers were produced by forcing water vapour to flow over a cold snow surface. The surface hoar crystals were then covered with a layer of sieved new snow, which was again left to sinter for at least one day. Fig. 1 schematically shows the experimental setups for producing the weak layers while Fig. 2 shows the resulting snow crystals.

In addition to classifying the snow types according to the International Classification for Seasonal Snow on the Ground (Fierz et al., 2009), we performed snow micro-penetrometer (SMP) measurements for characterizing the snow samples (Johnson and Schneebeli, 1999).

2.2. Force-controlled loading apparatus

The loading apparatus (Fig. 3) was designed to mimic loading conditions found in a natural snowpack. The relation between shear and normal force was determined by the "slope angle", which had a range of 0–60°. The maximum size of the snow samples that could be tested with the apparatus was 0.2 m × 0.1 m × 0.15 m (length × width × height). Prior to loading, the snow sample was frozen onto the lower sample holder which was tilted by an angle α and had been heated with a heating fan. Then the upper sample holder was heated and placed on top of the snow sample. The loading of the upper sample holder was achieved by draining fluid (i.e. alcohol) from a container placed on top of the shear apparatus into a container placed below the snow sample and attached to the upper sample holder. In order to avoid a moment of force on the weak layer, the upper sample holder was constructed T-shaped, and the weight was attached at its center of mass, so that the point of application of the load was at the weak layer (see Fig. 3). In Fig. 3b the weak layer is faintly visible on the right side of the sample at the height of the red cross which marks the center of gravity of the upper sample holder. The weight of the upper sample holder was compensated with a balanced weight, which was also

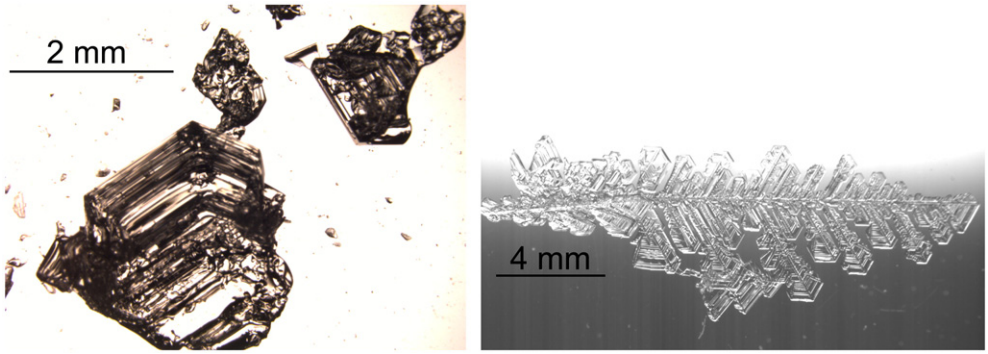

Fig. 2. Artificially produced depth hoar crystal (left) and artificially produced surface hoar crystal (right, photo: C. Mitterer).

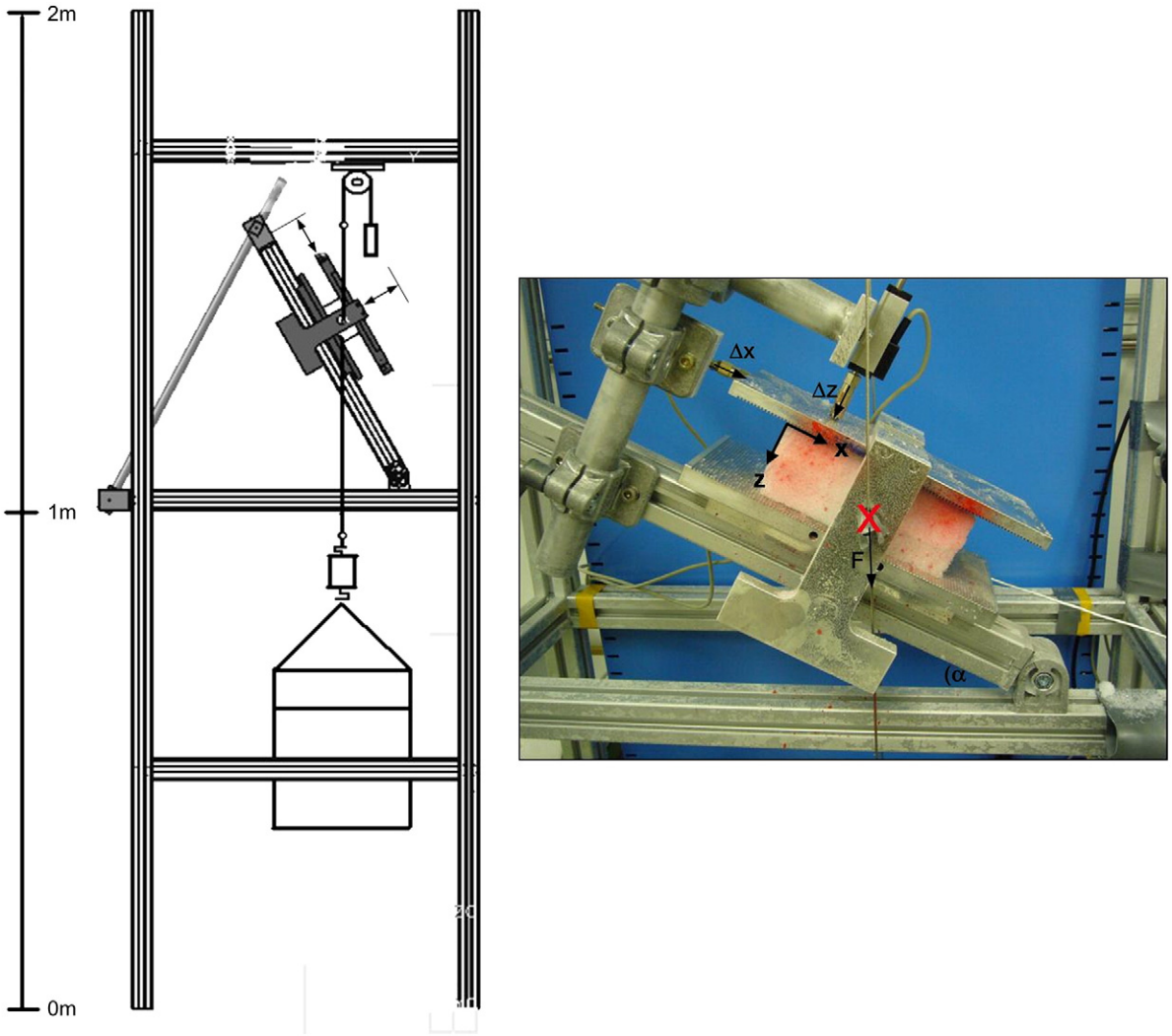

Fig. 3. Schematic of the new loading apparatus and photograph of a snow sample in the apparatus. α denotes the slope angle, F is the force acting on the snow sample, and Δz and Δx denote the compressive and shear displacement of the upper plate.

attached to the center of mass. The loading rate could be varied from 0.01 N s^{-1} (representing snowfall) to 5 N s^{-1} (representing rapid loading), and the maximum possible load was 180 N.

The force acting on the sample, i.e. the weight of the drained liquid, was measured with a force sensor (BGI sensor) positioned below the snow sample, with a maximum range of 250 N and an accuracy of $\pm$0.1 N. The signal from the force sensor was recorded with a sampling rate of 65 Hz.

The displacements of the upper sample holder, in slope parallel and slope normal direction, were measured with displacement sensors. The sensors were conductive-plastic resistance sensors (T 25 from Novotechnik) with a range of 30 mm and an accuracy of *pm* 0.01 mm. The signals from the displacement sensors were recorded with a data acquisition card (DAQCard-1200) from National Instruments with a sampling rate of 25 kHz.

2.3. Particle velocimetry method

The displacement field on the side of the snow sample was visualized with a particle image velocimetry algorithm (PIV). Assuming plane strain conditions, the displacement field on the side of the sample is representative for the displacement field also within the sample. The PIV algorithm recognizes patterns on a photograph taken from the snow sample and tracks them over various subsequent photographs. The snow sample was sprayed with paint to achieve sufficient contrast for the PIV algorithm to find a pattern. With a

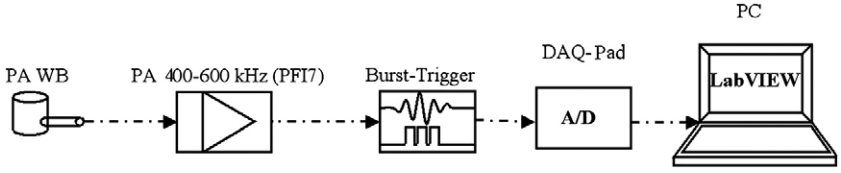

Fig. 4. Acoustic emission setup.

Table 1
Properties of the two types of snow samples. The snow type is characterized by grain type, grain size (mm), and hand hardness index according to Fierz et al. (2009).

Name	Type	Area (Length × width) (mm × mm)	Density (kg m^{-3})	Height (mm)	Snow type
H1	Homogeneous	120 × 70	270	48	RG, 0.5, 2
L1	Layered	125 × 70	280	28	RG, 0.5, 2
			–	1	FC(DH), 1, 1
			280	46	RG, 0.5, 2

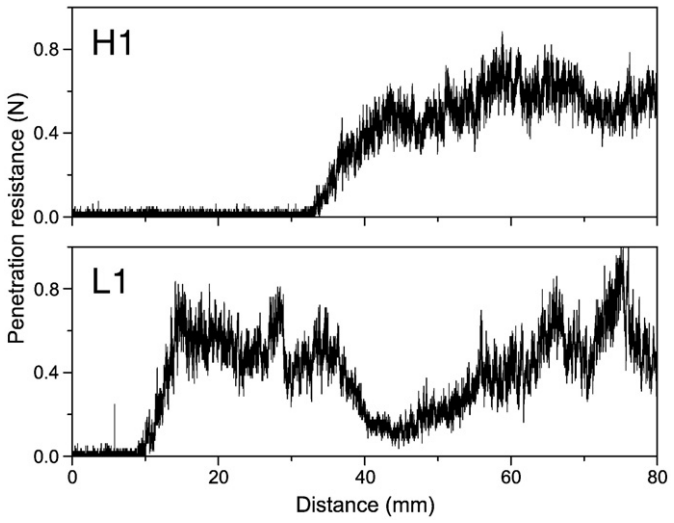

Fig. 5. Penetration resistance measurements of the samples H1 (top) and L1 (bottom) described in Table 1.

resolution of 1936 × 1288 pixels the maximum image rate was one image every two seconds. By comparing a sequence of images taken at different times during the experiment, the displacement, strain, and path lines were calculated Roesgen and Totaro, 1995. Before applying the algorithm to snow, we performed a parameter study to find the optimal parameter setting for our measurements. For the optimal parameter and our camera setup, the accuracy of displacement calculated by the algorithm was about ± 0.01 mm.

2.4. Acoustic emission measurement system

During the loading experiments acoustic emission (AE) signals were recorded. The acoustic measurement setup is shown in Fig. 4. The piezoelectric transducers were mounted in the bottom plate of the sample holder, i.e. the sensor was directly frozen to the snow. The AE sensor used in the experiments shown below was a wide band (WB) piezoelectric transducer (range 100 kHz–1 MHz) from Physical Acoustics (PA 1220B). The signal was amplified (by 60 dB) with a preamplifier (also from PA) which included a filter with a frequency range from 400 to 600 kHz. The purpose of the filter was to eliminate background noise from the coldroom cooling machine. The outcoming signal was fed into a burst-trigger circuit with a threshold of 150 mV and a dead time of 20 μs. The threshold level setting and the dead time allowed us to avoid triggering by background noise with low intensity and short disturbance signals. The optimal threshold and dead time were selected on the basis of preliminary experiments, where we used an oscilloscope to study the acoustic waveform (Ernst, 2009). If the acoustic signal exceeded the threshold the burst-trigger circuit emitted a pulse of length of the dead time. The pulses were recorded with a maximum sampling rate of 20 kHz. The pulses per time give the acoustic count rate, which is a measure of the intensity of the acoustic activity. A similar setup was already used by Scapozza et al. (2004) who studied the acoustic emission response of snow under compression.

3. Results and discussion

For the experiments shown here we used two different types of samples: homogeneous and layered. Both types of samples were produced in the cold laboratory. The homogeneous sample consisted of only one layer (small rounded grains: RG), while the layered sample consisted of three layers, which are characterized layer by layer (small rounded grains on top and at the bottom and a weak layer of faceted crystals (FC) and some depth hoar (DH) in between). An overview of the samples' properties is given in Table 1. Fig. 5 shows penetration resistance measurements of the samples. Although the weak layer is only 1 mm thick, the drop of force in the SMP signal is clearly visible but wider due to the extent of the SMP's force measuring cone which is 4.3 mm long. The tilt angle α of the loading apparatus was fixed to 26°, and the laboratory temperature was −6 °C.

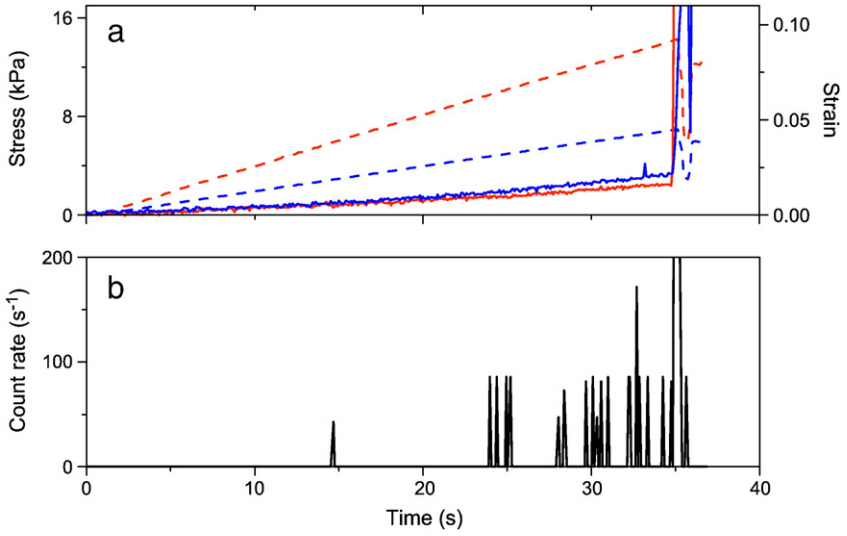

Fig. 6. (a) Compressive stress (red dashed curve), shear stress (blue dashed curve), compressive strain (red curve), shear strain (blue curve), and (b) acoustic emissions (count rate) measured during a loading experiment with a homogeneous snow sample (H1, Table 1).

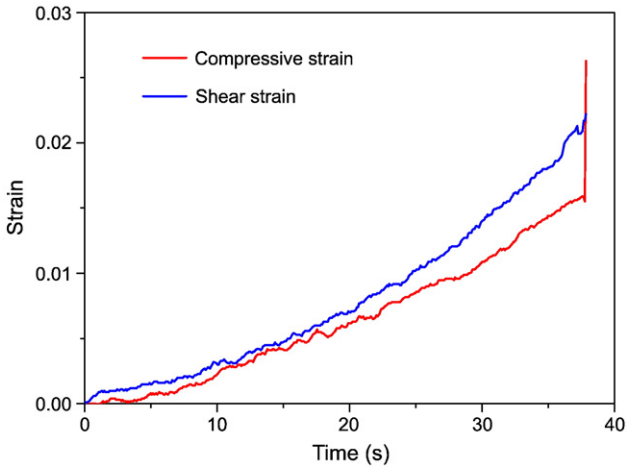

Fig. 7. Compressive and shear strain for the experiment with the homogeneous sample (Fig. 6), but before the huge increase of strain at fracture.

3.1. Load and displacement (stress and strain)

Typical stress and strain curves during a loading experiment with a homogeneous sample (H1, see Table 1) can be seen in Fig. 6. Normal and shear stress components were calculated from the load measurements (load divided by sample area). Compressive and shear strain were obtained from displacement measurements at the upper sample holder divided by sample height. We use a sample-based coordinate system, as shown in Fig. 3b. The sample was loaded with a constant loading rate, 0.4 kPa s^{-1} in compression and 0.2 kPa s^{-1} in shear. Catastrophic failure happened after $t=38$ s with a compressive and shear stress at fracture of $\sigma_{c,f}=14$ and $\sigma_{s,f}=7$ kPa, respectively. The strain in z-direction (see Fig. 3) was purely compressive, and the shear strain (in x-direction) was in "slope downward" direction. Both strain curves stay constant after fracture, and the shear strain curve displays a drop of strain during fracture, but these are artefacts due to the limited range of the displacement sensors and the movement of the upper sample holder during fracture, respectively. The compressive and shear strain on a larger scale can be seen in Fig. 7. The roughness of the curves is due to vibrations of the apparatus during the drainage of the alcohol into the lower container. Although the stress rates were constant, the strain rates increased, i.e. the material progressively weakened during the loading process.

For comparing our results to previous experiments, we calculated the average shear strain rate which was 5.6×10^{-4} s^{-1}. The shear stress (stress$\times\sin(\alpha)$) at fracture was 7 kPa and the shear strain 0.02. This is in remarkable accordance to what Schweizer (1998) found in his displacement-controlled shear experiments with homogeneous fine-grained snow.

The compressive stress, shear stress, compressive strain, and shear strain of an experiment with a layered sample (L1, see Table 1) are shown in Fig. 8. Qualitatively, the results look similar as in the experiment with the homogeneous sample. The sample fractured earlier, though, at $t=12$ s and at much smaller stresses, $\sigma_{c,f}=4$ kPa and $\sigma_{s,f}=2$ kPa. The applied compressive and shear stress rates were 0.4 kPa s^{-1} and 0.2 kPa s^{-1}, respectively.

3.2. PIV measurements

Fig. 9 shows the displacement within the homogeneous sample between two photographs taken at 4 and 10 seconds before fracture, respectively. It can be seen that the strain was spread equally over the whole sample, i.e. the displacement gradients $(\frac{\partial\Delta x}{\partial z})=3.5\times10^{-3}$ and $(\frac{\partial\Delta z}{\partial z})=3.0\times10^{-3}$ were constant.

Fig. 10a shows a photograph of the layered sample in the loading apparatus. The rectangle (35 mm$\times$63 mm) marked on the sample indicates the section which was used for the PIV analysis. The displacement field in the center of this rectangle can be seen in Fig. 10b. The weak layer was located parallel to the sample holders (x-direction) and its z-position was between 0 and -1 mm. Again we compared two photographs taken at 4 and 10 s before fracture. Clearly, the strain was concentrated within the weak layer, where we locally measured a displacement gradient of 3×10^{-2} in both shear and compression, while it was around 2×10^{-4} elsewhere. This gives a shear strain rate of 5×10^{-3} s^{-1} within the weak layer, while the global shear strain rate was only about 2×10^{-4} s^{-1}. This concentration of deformation (strain) in weak snowpack layers has often been assumed but has not been measured so far.

3.3. Acoustic emissions

During the loading experiment with the homogeneous sample, the acoustic count rate (Fig. 6b) increased shortly before fracture, this was

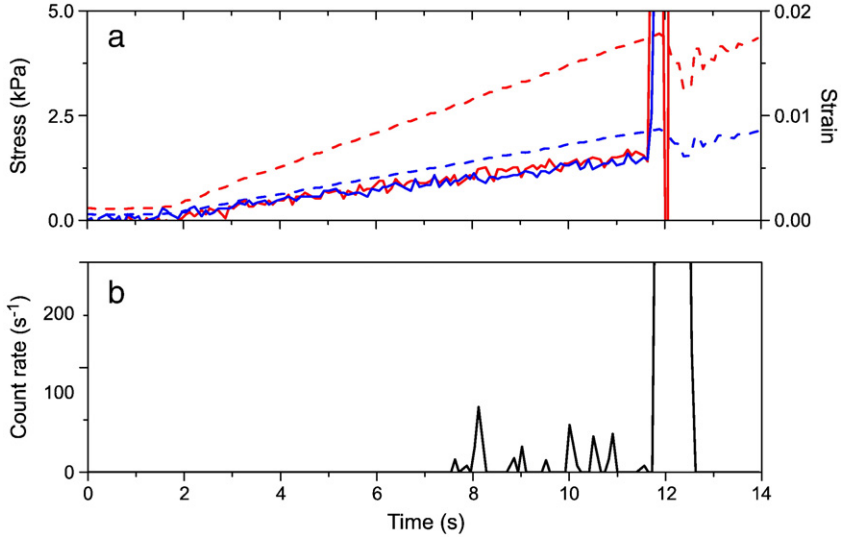

Fig. 8. (a) Compressive stress (red dashed curve), shear stress (blue dashed curve), compressive strain (red curve), shear strain (blue curve), and (b) acoustic emissions (count rate) measured during a loading experiment with a layered snow sample (L1, Table 1).

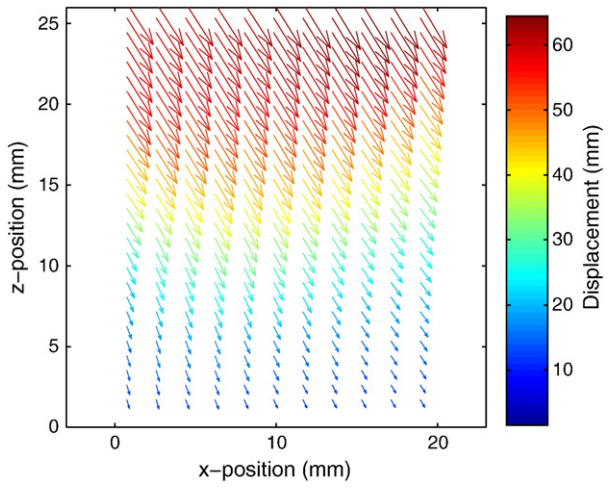

Fig. 9. Displacement field on the side of the homogeneous snow sample obtained by PIV analysis during the loading experiment (Fig. 6).

also observed in other experiments performed with homogeneous samples (Ernst, 2009). Acoustic emissions are presumed to be a measure of the number of bonds breaking between the snow grains during deformation. The non-linear increase in strain (Fig. 7) indicates that the material progressively weakened during deformation, and the AE may be an indicator of this weakening process.

Also for the layered sample we measured an increase in acoustic counts shortly before and, of course, at fracture (Fig. 8b). The count rate was smaller than in the case of the homogeneous sample, which can be easily understood if one considers that we were dealing with a weak layer, which had fewer bonds to break than a strong homogeneous sample. The repeated occurrence of acoustic counts shortly before fracture supports the hypothesis that acoustic emission signals may act as precursors to global failure within snow samples and may therefore also be useful as precursors to avalanche release. Still, this hypothesis needs to be tested with further experiments, which should be possible with the experimental setup presented here.

4. Conclusions and outlook

We have developed a loading apparatus with a measuring system to study the processes that lead to catastrophic fracture of layered snow samples with respect to dry-snow slab avalanche release. In our loading apparatus, the snow sample is loaded under nature-like conditions, i.e. it is tilted by a "slope angle" and is thereby loaded in shear and compression simultaneously. The advantage of this setup is clearly its resemblance to the processes occurring in nature, and therefore the relevance of the measurements performed for the release of slab avalanches. Until now, a simultaneous loading in shear and compression under controlled laboratory conditions had not been possible. A possible disadvantage of our setup might be, that its uniqueness makes exact comparison to other (laboratory) experiments with snow or to standard experiments with other materials difficult. Yet the order of magnitude of e.g. the fracture stress we measure for the homogeneous samples is the same as Schweizer (1998) found in his deformation-controlled shear experiments with homogeneous snow.

We demonstrated the capability of the system by showing exemplary results of two experiments with a homogeneous and a layered snow sample. We measured the stress, the global strain (compressive and shear), the displacement on the side of the snow samples, and recorded acoustic emissions. Using PIV we measured, for the first time, the concentration of strain within a weak layer that is subjected to a constant loading rate. As the samples weakened before fracture, the AE count rate increased, indicating that the AE may hint on the micro-mechanics during loading and serve as precursors to catastrophic failure.

In the future, we will perform more measurements of displacement and acoustic emissions during loading experiments with snow samples containing a weak snow layer, also to quantify the qualitative results shown here. The aim of these experiments will be 1) to study the deformation within the snow samples depending on the properties of the single layers and 2) to relate the acoustic emission measurements to the failure behaviour of the snow samples and manifest their nature as precursors to snow failure.

Acknowledgements

We especially thank Hans-Jürgen Herrmann for helpful discussions. The authors also thank Thomas Rösgen for providing the PIV algorithm we used for our analysis. Additionally, we acknowledge the work of Thomas Huber, who performed preliminary PIV measurements with snow during his B.S. thesis. Furthermore, we would like to thank Alec van Herwijnen for help with improving this paper. Funding was provided by the Swiss National Science Foundation (no. 200021-

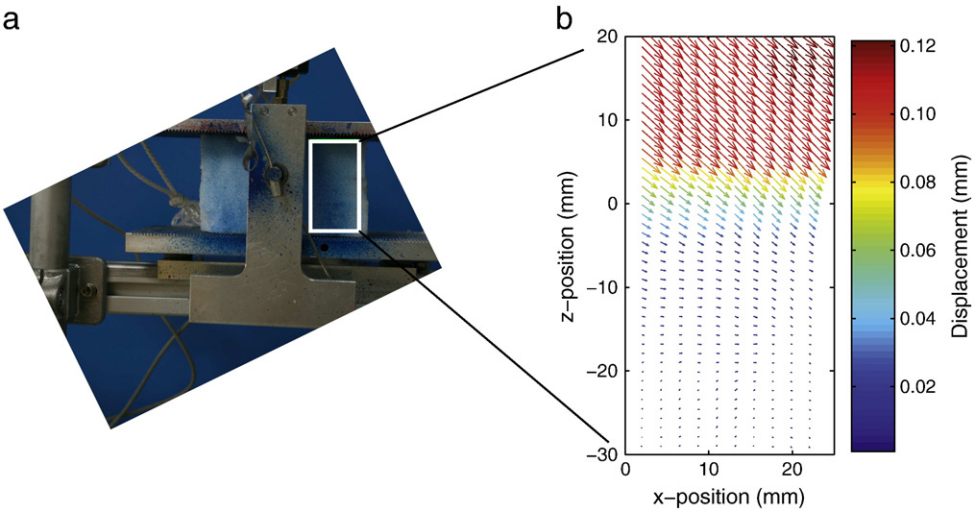

Fig. 10. (a) Photograph of the layered snow sample during the loading experiment (Fig. 8) with the section marked which was used for the PIV analysis. (b) Displacement field on the side of the layered snow sample derived with PIV.

109366). This work also profited from collaborations within the FP6 project TRIGS (European Commission) and the CCESproject TRAMM (ETH Board).

References

Borstad, C., McClung, D., 2004. Slab fracture at 1900 frames per second — experimental methods. In: Elder, K. (Ed.), Proceedings ISSW 2004: International Snow Science Workshop. Jackson Hole, Wyoming, USA, 19–24 September 2004, pp. 22–24.

Camponovo, C., Schweizer, J., 2001. Rheological measurements of the viscoelastic properties of snow. Annals of Glaciology 32, 44–50.

Cole, D., Dempsey, J., 2004. In situ sea ice experiments in McMurdo Sound: cyclic loading, fracture, and acoustic emissions. Journal of Cold Regions Engineering 18, 155–174.

de Montmollin, V., 1982. Shear tests on snow explained by fast metamorphism. Journal of Glaciology 28 (98), 187–198.

Ernst, R., 2009. Akustische Emissionen von Schnee bei kraftgesteuerten Scherversuchen. M.S. thesis, ETH Zurich, Switzerland.

Fierz, C., Armstrong, R., Durand, Y., Etchevers, P., Greene, E., McClung, D., Nishimura, K., Satyawali, P., Sokratov, S., 2009. The International Classification for Seasonal Snow on the Ground. : (IHP-VII Technical Documents in Hydrology), 83. UNESCO-International Hydrological Program, Paris. 90 pp.

Fukuzawa, T., Narita, H., 1993. An experimental study on the mechanical behavior of a depth hoar layer under shear stress. Proceedings International Snow Science Workshop. Breckenridge, Colorado, U.S.A., 4–8 October 1992, pp. 171–175.

Gleason, J., 2004. Particle image velocimetry; a new technique to measure strain in loaded snow. In: Elder, K. (Ed.), Proceedings ISSW 2004. International Snow Science Workshop. Jackson Hole, Wyoming, USA, 19–24 September 2004, pp. 44–49.

Jamieson, B.J., Schweizer, J., 2000. Texture and strength changes of buried surface-hoar layers with implications for dry snow-slab avalanche release. Journal of Glaciology 46 (152), 151–160.

Johnson, J., Schneebeli, M., 1999. Characterizing the microstructural and micromechanical properties of snow. Cold Regions Science and Technology 30 (1–3), 91–100.

Joshi, S., Mahajan, P., Upadhyay, A., 2006. Study of layered snow under shear and tension. In: Gleason, A. (Ed.), Proceedings ISSW 2006. International Snow Science Workshop. Telluride, Colorado, USA, 1–6 October 2006, pp. 165–173.

McClung, D., 1977. Direct simple shear tests on snow and their relation to slab avalanche formation. Journal of Glaciology 19 (81), 101–109.

McClung, D., 1987. In: Salm, B., Gubler, H. (Eds.), Mechanics of snow slab failure from a geotechnical perspective. : Symposium at Davos 1986 — Avalanche Formation, Movement and Effects, No. 162. IAHS Publ., pp. 475–508.

Meier, M., 2006. Produktion von naturidentischem Schnee. M.S. thesis, ETH Zurich, Switzerland.

Podolsky, E., Chernous, P., Abe, O., Barashev, N., Nishimura, K., 2008. Experimental study of short-term loading influence on shear strength. In: Campbell, C., Conger, S., Haegeli, P. (Eds.), Proceedings International Snow Science Workshop. Whistler B.C., Canada, 21–27 September 2008, pp. 701–708.

Roesgen, T., Totaro, R., 1995. Two-dimensional on-line particle imaging velocimetry. Experiments in Fluids 19 (3), 188–193.

Scapozza, C., Bucher, F., Amann, P., Ammann, W., Bartelt, P., 2004. The temperature- and density-dependent acoustic emission response of snow in monoaxial compression tests. Annals of Glaciology 38, 291–298.

Schweizer, J., 1998. Laboratory experiments on shear failure of snow. Annals of Glaciology 26, 97–102.

Schweizer, J., Jamieson, J., Schneebeli, M., 2003. Snow avalanche formation. Reviews of Geophysics 41 (4), 1016.

Sommerfeld, R.A., Gubler, H., 1983. Snow avalanches and acoustic emissions. Annals of Glaciology 4, 271–276.

St. Lawrence, W., 1980. The acoustic emission in snow. Journal of Glaciology 26 (94), 209–216.

van Herwijnen, A., Jamieson, B., 2005. High speed photography of fractures in weak snowpack layers. Cold Regions Science and Technology 43 (1–2), 71–82.

van Herwijnen, A., Schweizer, J., 2008. Continuous monitoring of acoustic emissions in an avalanche start zone. Geophysical Research Abstracts 10 EGU2008-A-09762.